

ESTIMATING MAXIMUM AIR TEMPERATURE IN KHOOZEZTAN PLAIN USING NOAA SATELLITE IMAGES DATA AND ARTIFICIAL NEURAL NETWORK

Ali Rahimi Khoob

Assistant Professor, Irrigation and Drainage Engineering Department

Faculty of Agricultural Engineering, College of Aboureyhan

University of Tehran, Iran

Tel: (98)-292-3025366 Fax: (98)-292-3025366

Email: akhob@ut.ac.ir

KEY WORDS: Air temperature, NOAA satellite, neural network, Remote sensing

ABSTRACT: Air temperature prediction models using satellite data are based on the two variables of land surface temperature and vegetation cover index. These variables are obtained by effecting atmospheric corrections in the values for the above data. The data of water vapor, ozone, and atmospheric aerosol optical depth are required for the atmospheric correction of visible bands. However, no measurements are available for these parameters in most locations of Iran. Using the common methods, land surface temperature can be measured accurately within 2°C. Given these limitations, efforts are made in this study to evaluate the accuracy of predicting maximum air temperature when uncorrected atmospheric data from the NOAA Satellite are used by a neural network. For this purpose, various neural network models were constructed from different combinations of data from 4 bands of NOAA satellite and 3 different geographical variables as inputs to the model in order to select the best model. The results showed that the best neural network was the one consisting of 6 neurons as the input layer (including 4 bands of NOAA satellite, day of the year, and altitude) and with 19 neurons in the hidden layer. In this structure, the statistical criteria of R^2 , RMSE, and CC were found to equal 0.62, 1.72°C, and 0.78 respectively.

1. INTRODUCTION

Maximum air temperature (T_{max}) is needed for understanding climate, evapotranspiration estimation and environmental assessment. The density of the station network is often not sufficient when air temperature is employed in regional study. Satellite remote sensing provides better spatial coverage than do surface meteorological data.

There are two methods by which the air temperature from satellite images is estimated. One is surface temperature/spectral vegetation index (TVX) method developed by Czajkowski et al. (1997) and Prihodko and Goward (1997). Another is empirical equation derived from statistical results for estimating air temperature (Cresswell et al., 1999). The TVX method is based on the similarity between the air temperature close to the vegetation canopy and the temperature of the vegetation canopy.

For the surface temperature estimation, numerous split-window algorithms have been developed by authors using data from two thermal infrared bands located at 11 μm and 12 μm (channels 4 and 5 of AVHRR sensor). It is difficult to retrieve the surface temperature precisely because the measurement of thermal infrared radiance is affected by atmospheric absorption (water vapor and other gases). The split-window algorithms have proved very successful for dealing with atmospheric effects. Over the oceans, where the emissivity is constant and close to one, this technique gives sea surface temperatures within 1 °K of those observed (McLain et al., 1985). Over land, however, emissivity is highly variable and needs to be included in the methodology. The accuracy of split-window algorithms depends on the magnitude of the difference between

the two ground emissivities in the bands (Becker, 1987). Unfortunately, the ground emissivity cannot be derived from satellite images. The best achievable accuracy of LST is less than $\pm 2^\circ\text{C}$ for flat terrain with relatively dry atmospheres, and it would be possible to get emissivity maps with an accuracy of 1% (Sobrino et al. 1991, Coll et al. 1994, Qin and Karnieli 1999). Air temperature is more difficult to determine from remotely sensed data, because of its strong dependence on the surface properties that vary significantly both in space and time (Voogt and Oke, 1997). The TVX and the empirical methods have provided estimated air temperatures with an RMS error of 3°C .

The variable of vegetation cover index that used for prediction of air temperature models are obtained by effecting atmospheric corrections. The data of Water vapor, ozone, and atmospheric aerosol optical depth are required for the atmospheric correction of visible bands. However, no measurements are available for these parameters in most locations of Iran. Given these limitations, efforts are made in this study to evaluate the accuracy of predicting T_{\max} when uncorrected atmospheric data from the NOAA Satellite are used by a neural network. The basic goal of this study is to examine whether it is possible to attain better accuracy of air temperature from satellite images than that achieved in previous methods by ANNs

2. MATERIALS AND METHODS

2.1 Study Area

The area under study was the Khuzestan plain, which lies approximately between 29.95 and 32.9°N in latitude and between 47.6 and 50.6°E in longitude. This plain is in the southwest of Iran and covers an area of $63,238\text{ km}^2$. Khuzestan plain is categorized as a semiarid climate based on the Koppen climate classification. Measured daily T_{\max} from 9 meteorological stations spread throughout the study area were used as actual data for develop ANN model for this study. The stations belong to the meteorological organization of Iran and cover most of the plain. The spatial distributions of selected stations are presented in Figure 1.

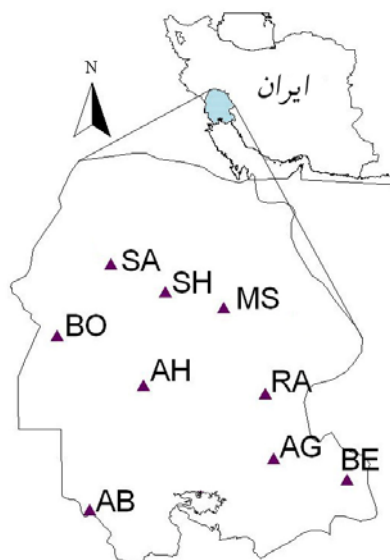


Figure 1: Spatial distribution of the 9 meteorological stations used in the study.

2.2 Satellite data

A total of 365 images without cloud cover of NOAA-14 AVHRR level 1b, covering the plain of Khuzestan in Iran were collected from the Satellite Active Archive (SAA) of NOAA. These images were between May and September from 1997 to 2003 that were scanned between 12 Noon and 4 PM (local time), therefore were suited to estimate T_{max} . At a first step, the images were radiometrically and geometrically corrected. The data in the digital counts were converted to reflectance (for channels 1 and 2) and to brightness temperatures (for the thermal channels 4 and 5) using the calibration information given in the documentation for each image. Converted data are average within a 3×3 pixels size area (corresponding to 3×3 km²) centered on the station of interest. In this study, different combinations from these averages of four bands of AVHRR images were employed together with the value of altitude (AL), solar zenith angle (SZA) and Julian day (JD) as inputs to the networks for estimating T_{max} .

2.3 Artificial neural network

To estimate maximum air temperature from the readily available meteorological data, we used multi-layer perceptron (MLP) neural networks that consist of one input layer, one hidden layer and one output layer using sigmoid transfer functions. The transfer function in the networks was log-sigmoid for this paper. The accuracy of the networks was evaluated for each epoch in the training through mean squared error (MSE). The backpropagation (BP) algorithm was employed to train our MLP neural network. In this study, all the data was divided into three sets. The first set is the training set for determining the weights and biases of the network. The second set is the validation set for evaluating the weights and biases and for deciding when to stop training. The last data set is for validating the weights and biases to verify the effectiveness of the stopping criterion and to estimate the expected network operation on new data sets.

3. RESULTS

In the first attempt in this study, the various combinations of four bands of AVHRR (B1, B2, B4 and B5) were directly selected as input variables to the networks for estimating T_{max} . The number of hidden layer nodes was fixed at 10 for all runs. The statistical results are given in table 1. It can be seen that the thermal bands 4 and 5, which are used for retrieving surface temperature, were significant variables related to T_{max} . The highest correlation coefficient (CC=0.58) was obtained, when four bands of AVHRR image (4B) were used as inputs.

Table 1. Statistical results of the networks trained with various inputs using the four bands of AVHRR image

| Input Data | RMSE (°C) | R ² | CC | MBE (°C) |
|--------------|--------------|----------------|------|-------------|
| B1 | 2.86 | 0.01 | .01 | .06 |
| B2 | 2.86 | .01 | .07 | .09 |
| B1 , B2 | 2.59 | .02 | 0.14 | 0.0 |
| B4 | 2.33 | 0.28 | 0.53 | 0.05 |
| B5 | 2.41 | 0.25 | 0.50 | 0.02 |
| B4 , B5 | 2.32 | 0.34 | 0.55 | 0.06 |
| B1, B4, B5 | 2.31 | 0.33 | 0.56 | 0.04 |
| B2,B4,B5 | 2.32 | 0.33 | 0.54 | 0.01 |
| B1,B2,B4, B5 | 2.21 | 0.36 | 0.58 | 0.08 |

In the second attempt, the neural networks were trained using various combinations of four AVHRR bands (4B) with altitude, solar zenith angle, and Julian day. The number of hidden nodes was fixed at 10 for all networks. The results of statistical comparison are summarized in Table 2. The results indicated that, adding geographic variables will increase accuracy and the correlation coefficient of networks. The best accuracy was obtained, when we used four bands, altitude and Julian day (4B, JD, AL) as input variables.

Table 2. Statistical results of the networks trained with various inputs combinations of four AVHRR bands (4B), altitude (AL), Julian day (JD) and solar zenith angle (SZA)

| Input data | RMSE (°C) | R ² | CC | MBE (°C) |
|-----------------|--------------|----------------|------|-------------|
| 4B, AL | 2.07 | 0.49 | 0.66 | -0.01 |
| 4B, JD | 1.87 | 0.54 | 0.73 | -0.04 |
| 4B, SZA | 2.15 | 0.45 | 0.63 | 0.04 |
| 4B,JD, AL | 1.72 | 0.62 | 0.78 | -0.01 |
| 4B,AL,SZA | 1.99 | 0.53 | 0.69 | 0.03 |
| 4B, JD, SZA | 1.79 | 0.57 | 0.76 | 0.01 |
| 4B, AL, JD, SZA | 1.81 | 0.58 | 0.75 | 0.02 |

The number of nodes in the hidden layer was determined by trial and error. The neural networks were trained using four bands, altitude and Julian day (4B, JD, AL) with from one to 30 hidden nodes. After each training run, RMSE, CC and R² were calculated using only the test data set to find the optimal number of hidden nodes. Figure 2 shows the effect of changing the number of nodes in hidden layer on the network accuracy. It is clear that this factor had a significant bearing on the network accuracy. The best CC, RMSE and R² (0.78, 1.72 °C and 0.62 respectively) was also found with 19 nodes.

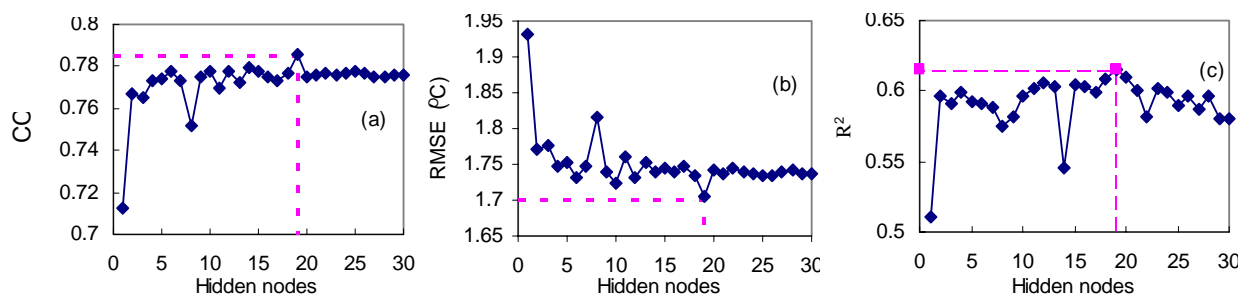


Figure 2. Relation between accuracy of ANN and the number of nodes for estimating T_{max} . (a) Correlation coefficients (b) RMSE and (c) R².

4. Conclusion

In this paper, efforts were made to evaluate the accuracy of predicting T_{max} when uncorrected atmospheric data from the NOAA Satellite are used by a neural network. T_{max} was estimated using the four bands of AVHRR, altitude, solar zenith angle, and Julian day. The best accuracy was obtained, when we used four bands of AVHRR, altitude and Julian day (4B, JD, AL) as input variables with 19 hidden nodes. The RMSE, cc and R² were about 1.72 °C, 0.78 and 0.62 respectively.

Acknowledgment

The author would like to express his sincere gratitude to Department of Irrigation and Drainage Engineering, University collage of Aboureyhan and University of Tehran. The research described in this paper was supported with funds provided by University of Tehran.

References

- Becker, F., 1987. The impact of spectral emissivity on the measurement of land surface temperature from a satellite. *International Journal of Remote Sensing*, 8, pp. 1509-1522.
- Cazjkowski, K. P., Mulherm, T., Goward, S. N., Cihlar, J., Dubayah, R. O. and Prince., S. D., 1997. Biospheric environmental monitoring at Boreas with AVHRR observation. *Journal of Geophysical Research*, 102, pp. 29651-29662.
- Coll, C., Caselles, V. and Schmugge, T. J., 1994. Estimation of land surface emissivity differences in the split-window channels of AVHRR. *Remote Sensing of Environment*, 48, pp. 127-134.
- Cresswell, M. P., Morse, A. P., Thomson, M. C., and Connor, S. J., 1999. Estimating surface air temperatures, from Meteosat land surface temperatures, using an empirical solar zenith angle model. *International Journal of Remote Sensing*, 20, pp. 1125-1132.
- McLain, E.P., Pichel, W.G. and Walker, C.C., 1985. Comparative performance of AVHRR-based multichannel sea surface temperatures. *Journal of Geophysical Research* 90, pp. 11587–11601.
- Prihodko, L. and Goward, S. N., 1997. Estimation of air temperature from remotely sensed surface observation. *Remote Sensing of Environment*, 60, pp. 335-346.
- Qin, Z., and Karnieli, A., 1999. Progress in the remote sensing of land surface temperature and ground emissivity using NOAA-AVHRR data. *International Journal of Remote Sensing*, 20, pp. 2367-2393.
- Sobrino, J. A., Coll, C. and Caselles, V., 1991. Atmospheric correction for land surface temperature using NOAA-11 AVHRR channels 4 and 5. *Remote Sensing of Environment*, 38, pp. 19-34.
- Voogt, J. A. and Oke, T. R., 1997. Complete urban surface temperatures. *Journal of Applied Meteorology*, 36 (9), pp. 1117–1132.